J Mater Sci: Mater Med (2014) 25:1737–1746
DOI 10.1007/s10856-014-5201-9

Antibacterial and bioactive calcium titanate layers formed on Ti metal and its alloys

Takashi Kizuki · Tomiharu Matsushita · Tadashi Kokubo

Received: 21 December 2013 / Accepted: 18 March 2014 / Published online: 29 March 2014

Abstract An antibacterial and bioactive titanium (Ti)-based material was developed for use as a bone substitute under load-bearing conditions. As previously reported, Ti metal was successively subjected to NaOH, $CaCl_2$, heat, and water treatments to form a calcium-deficient calcium titanate layer on its surface. When placed in a simulated body fluid (SBF), this bioactive Ti formed an apatite layer on its surface and tightly bonded to bones in the body. To address concerns regarding deep infection during orthopedic surgery, Ag^+ ions were incorporated on the surface of this bioactive Ti metal to impart antibacterial properties. Ti metal was first soaked in a 5 M NaOH solution to form a 1 μm-thick sodium hydrogen titanate layer on the surface and then in a 100 mM $CaCl_2$ solution to form a calcium hydrogen titanate layer via replacement of the Na^+ ions with Ca^{2+} ions. The Ti material was subsequently heated at 600 °C for 1 h to transform the calcium hydrogen titanate into calcium titanate. This heat-treated titanium metal was then soaked in 0.01–10 mM $AgNO_3$ solutions at 80 °C for 24 h. As a result, 0.1–0.82 at.% Ag^+ ions and a small amount of H_3O^+ ions were incorporated into the surface calcium titanate layers. The resultant products formed apatite on their surface in an SBF, released 0.35–3.24 ppm Ag^+ ion into the fetal bovine serum within 24 h, and exhibited a strong antibacterial effect against *Staphylococcus aureus*. These results suggest that the present Ti metals should exhibit strong antibacterial properties in the living body in addition to tightly bonding to the surrounding bone through the apatite layer that forms on their surfaces in the body.

T. Kizuki (✉) · T. Matsushita · T. Kokubo
Department of Biomedical Sciences, College of Life and Health Sciences, Chubu University, 1200 Matsumoto-cho, Kasugai, Aichi 487-8501, Japan
e-mail: t-kizuki@isc.chubu.ac.jp

1 Introduction

Titanium (Ti) metal and its alloys have been widely used as orthopedic and dental implants due to their high fracture toughness and good biocompatibility. However, they do not bond to living bones. Previously, we showed that even Ti metal and its alloys form an apatite layer on their surfaces in the living body and bond to surrounding living bone through this apatite layer, if they are first subjected to NaOH and heat treatment to form a sodium titanate layer [1–3] or to NaOH, $CaCl_2$, heat, and water treatment to form a calcium-deficient calcium titanate layer [4–6] on their surfaces. These methods have been applied to the generation of bioactive, porous Ti metal surfaces in a total artificial hip joint that has been used with clinical success in Japan since 2007 [7, 8].

However, deep infection still remains a serious problem associated with orthopedic surgery. It has been reported that deep infections typically occur in 1–2 % of patients that have received total hip arthroplasties [9]. When deep infection occurs, removal and reimplantation of the implant is often necessary, which places additional undesired stress on the patient. Therefore, Ti metal and Ti alloys are required not only to exhibit bone-bonding ability, but also to exhibit antibacterial activity.

It has been reported that bioactive Na_2O–CaO–SiO_2–P_2O_5 glasses exhibit antibacterial activity without addition of any antibacterial agent [10]. Their native antibacterial activity is attributed to the alkaline environment resulting from the release of Na^+ ions from the glasses [11]. Therefore, if coated with such a bioactive glass, Ti metal

and its alloys should exhibit antibacterial activity. However, unfortunately, these bioactive glass layers are not stable in the body for a sufficient period of time.

The application of bioactive glass and hydroxyapatite layers containing silver ions on metals has also been attempted using various methods such as precipitation from aqueous solutions [12], electrochemical deposition [13], sol–gel synthesis [14], sputtering [15], plasma spray [16], and thermal spray [17]. Apatite and calcium phosphate coatings containing antibiotics have also been reported [18]. However, foreign layers coated on metallic substrates are typically not stable in the living body for a long period of time.

Inoue et al. [19] attempted to form a silver-containing bioactive sodium titanate layer by soaking Ti metal that had been subjected to NaOH solution treatment or NaOH hydrothermal treatment in a silver acetate solution. The silver ions were successfully incorporated into the sodium titanate layer formed on the Ti metal, and the resultant product exhibited antibacterial activity. However, the silver ions also precipitated as metallic colloids on the surface of the Ti metal [20]. In addition, neither the apatite-forming ability nor the bone-bonding ability of the resultant product was reported.

In the present study, incorporation of silver ions into the calcium titanate layer formed on Ti metal and its alloy using chemical and heat treatments was attempted. The antibacterial activity and apatite-forming ability of the resultant products were evaluated in vitro, and their properties were compared with those of Ti metals formed with Ag-containing sodium titanate surface layers and those of Ti metals formed with Ag-free sodium titanate and calcium titanate layers.

2 Materials and methods

2.1 Sample preparation

Ti metal with a sodium titanate surface layer was prepared as previously reported [4]. Briefly, a $10 \times 10 \times 1$ mm^3 sample of pure Ti metal (>99.5 % and compliant with ISO5832-2. Nilaco Co., Japan) was polished with a 400 grit diamond disk and then washed sequentially with acetone, 2-propanol, and ultrapure water in an ultrasonic cleaner for 30 min each. Next, the Ti metal was soaked in a 5 M NaOH solution (5 ml) at 60 °C for 24 h and then gently washed with ultrapure water. The NaOH-treated Ti metal was subsequently heated to 600 °C at a rate of 5 °C/min, maintained at 600 °C for 1 h in an ambient atmosphere and then naturally cooled.

As a second reference material, Ti metal with a Ca-deficient calcium titanate surface layer was also prepared. The NaOH-treated Ti metal described above was soaked in a 100 mM $CaCl_2$ solution (10 ml) at 40 °C for 24 h and then gently washed with ultrapure water. It was subsequently heated at 600 °C using the same method described above. The NaOH-$CaCl_2$-heat-treated Ti metal was finally soaked in ultrapure water (10 ml) at 80 °C for 24 h.

Ti metal with an Ag-containing sodium titanate surface layer was then prepared. The NaOH-treated Ti metal prepared as described above was soaked in 0.01–1 mM $AgNO_3$ solutions (10 ml) at 40 °C for 24 h, gently washed with ultrapure water, and then heated at 600 °C using the same method as described above.

Ti metal with an Ag-containing calcium titanate surface layer was also prepared. The NaOH-$CaCl_2$-heat-treated Ti metal prepared as described above was soaked in 0.01–25 mM $AgNO_3$ solutions (10 ml) at 80 °C for 24 h instead of water, and then gently washed with ultrapure water.

Finally, a Ti–15Zr–4Nb–4Ta alloy (Kobe Steel, Ltd., Ti: Bal., Zr: 14.51, Nb: 3.83, Ta: 3.94, Pd: 0.16, O: 0.25 mass%) with an Ag-containing calcium titanate surface layer was prepared. The Ti–15Zr–4Nb–4Ta alloy was first soaked in a 5 M NaOH solution (5 ml) at 60 °C for 24 h and then in a 100 mM $CaCl_2$ solution (10 ml) at 40 °C for 24 h, followed by heating to 700 °C at a rate of 5 °C/min, at which temperature it was maintained for 1 h in an ambient atmosphere. Once cooled, this heat-treated alloy was soaked in a 1 mM $AgNO_3$ solution (10 ml) at 80 °C for 24 h.

2.2 Surface characterization

The surface morphology of the treated-Ti metals and alloy were examined using a field emission scanning electron microscope (FE-SEM, S-4300, Hitachi Ltd., Japan). The chemical composition of the surfaces of the samples was analyzed using an energy dispersive X-ray analyzer (EDX, EMAX-7000, Horiba Ltd., Japan) attached to the SEM. Measurements were conducted at 5 locations on one sample and averaged. The distribution of the elements as a function of the depth from the surface of the treated-Ti metals was determined via Auger electron spectroscopy (AES, PHI-670, ULVAC-PHI Inc., Japan). The phases of the surfaces of the treated-Ti metals and alloy were identified using a thin-film X-ray diffractometer (TF-XRD, RINT2500, Rigaku Co., Japan).

2.3 Evaluation of the apatite-forming ability

It has been previously shown that Ti metal in the living body that forms an apatite layer on its surface bonds to living bone through the apatite layer, and the apatite can be reproduced in an acellular simulated body fluid (SBF) with

an ion concentration nearly equal to that of human blood plasma [21]. Therefore, the ability of the Ti metals, which were prepared using different treatment methods, to form an apatite layer was evaluated. Specifically, a pH 7.40 simulated body fluid (SBF; ISO 23317) with Na^+, K^+, Mg^{2+}, Ca^{2+}, Cl^-, HCO_3^-, HPO_4^{2-}, and SO_4^{2-} concentrations of 142.0, 5.0, 1.5, 2.5, 147.8, 4.2, 1.0, and 0.5, respectively, was prepared by first dissolving reagent-grade NaCl, $NaHCO_3$, KCl, $K_2HPO_4{\cdot}3H_2O$, $MgCl_2{\cdot}6H_2O$, $CaCl_2$, and Na_2SO_4 in ultrapure water. This solution was then buffered at pH 7.40 using tris(hydroxymethyl)aminomethane ($(CH_2OH)_3CNH_2$) and a 1.0 M HCl aqueous solution at 36.5 °C [22]. The treated Ti metals and alloy were soaked in this SBF at 36.5 °C for 24 h, removed, and then rinsed with ultrapure water. Apatite formation on the sample surface was examined using FE-SEM and TF-XRD.

2.4 Measurement of Ag^+ ion release

The treated Ti metals and alloy were soaked in ultrapure water or fetal bovine serum (FBS, GIBCO®, Life Technologies Co., USA) at 36.5 °C several times for periods ranging from 1 to 24 h. The amount of Ag^+ ions released from the treated Ti metals and alloy were measured using inductively coupled plasma atomic emission spectroscopy (ICP, SPS3100, SII NanoTechnology Inc., Japan).

2.5 Evaluation of antibacterial activity

The antibacterial activity of the treated Ti metals and alloy was evaluated according to the International Standardization Organization (ISO) test 22196. A *Staphylococcus aureus* (*St. aureus*) suspension in 0.1 ml was dropped on a $25 \times 25 \times 1$ mm^3 treated Ti specimen and then covered with a 20×20 mm^2 polyethylene film. The inoculated specimens were placed in an incubator at 35 °C for 24 h. After incubation, each specimen was washed with a soybean casein digest broth containing lecithin and polyoxyethylene sorbitan monooleate (SCDLP broth, 20 ml) to recover the bacteria. The recovered suspension was placed in a petri dish with a plate count agar after tenfold serial dilutions and cultured at 35 °C for 48 h. After incubation, the number of colonies in the petri dish was counted, and the number of viable *St. aureus* was calculated using the number of colonies and the dilution factor. Finally, the antibacterial activity value (R) for each specimen was calculated as follows:

$$R = \{\log (B/A) - \log (C/A)\} = \log (B/C),$$

where A is the number of viable *St. aureus* recovered from the untreated specimen immediately after inoculation, B is the number of viable *St. aureus* recovered from the untreated specimen immediately after 24 h incubation, and C is the number of viable *St. aureus* recovered from the treated specimen immediately after 24 h incubation.

Table 1 Atomic concentrations at the surface of NaOH-heat and NaOH-$AgNO_3$-heat-treated Ti metals

Treatment	Concentration / at.%			
	Ti	O	Na	Ag
NaOH-heat	26.98 (0.54)	67.27 (0.27)	5.75 (0.38)	0.00 (0.00)
NaOH-0.01 mM $AgNO_3$-heat	30.17 (0.12)	67.57 (0.09)	1.48 (0.08)	0.78 (0.16)
NaOH-0.1 mM $AgNO_3$-heat	30.70 (0.25)	67.27 (0.06)	0.08 (0.08)	1.96 (0.26)
NaOH-1 mM $AgNO_3$-heat	30.75 (0.39)	67.37 (0.63)	0.00 (0.01)	1.89 (0.29)

Numbers in parentheses mean SD

3 Results

3.1 Surface structure

Table 1 lists the concentrations of the various elements present on the surfaces of the NaOH-heat-treated and NaOH-$AgNO_3$-heat-treated Ti metals. The concentration of sodium was 5.75 at.% on the surface of the Ti metal subjected to sequential NaOH and heat treatment. However, when the NaOH-treated Ti metal was soaked in a 0.01, 0.1, or 1 $AgNO_3$ solution and then heat-treated, the amount of sodium detected on the Ti surface decreased to 1.48, 0.08, and 0.00 at.%, while 0.78, 1.96, and 1.89 at.% silver was detected, respectively.

Figure 1 shows SEM images of the surfaces of Ti metals treated sequentially with NaOH and heat, and NaOH, $AgNO_3$, and heat. The Ti metal subjected to the NaOH and heat treatments had a uniform fine network structure on its surface, while after the final heat treatment, nanosized particles were observed on the fine network structure of the Ti metals soaked in both NaOH and $AgNO_3$ solutions, and the number of nanoparticles increased as the concentration of the $AgNO_3$ solution increased.

Figure 2 shows TF-XRD patterns of the surfaces of the NaOH-heat-treated and NaOH-$AgNO_3$-heat-treated Ti metals. Only sodium titanate and the rutile phase of TiO_2 were detected in addition to Ti metal on the surface of the sample subjected to sequential NaOH and heat treatments, while metallic silver was detected along with sodium titanate, rutile TiO_2, and Ti metal on the surfaces of the Ti metals subjected to sequential NaOH, $AgNO_3$, and heat treatments. Notably, the diffraction peaks ascribed to the sodium titanate shifted slightly to higher diffraction angles as the concentration of the $AgNO_3$ solution increased, most likely due to the incorporation of the silver ions. The

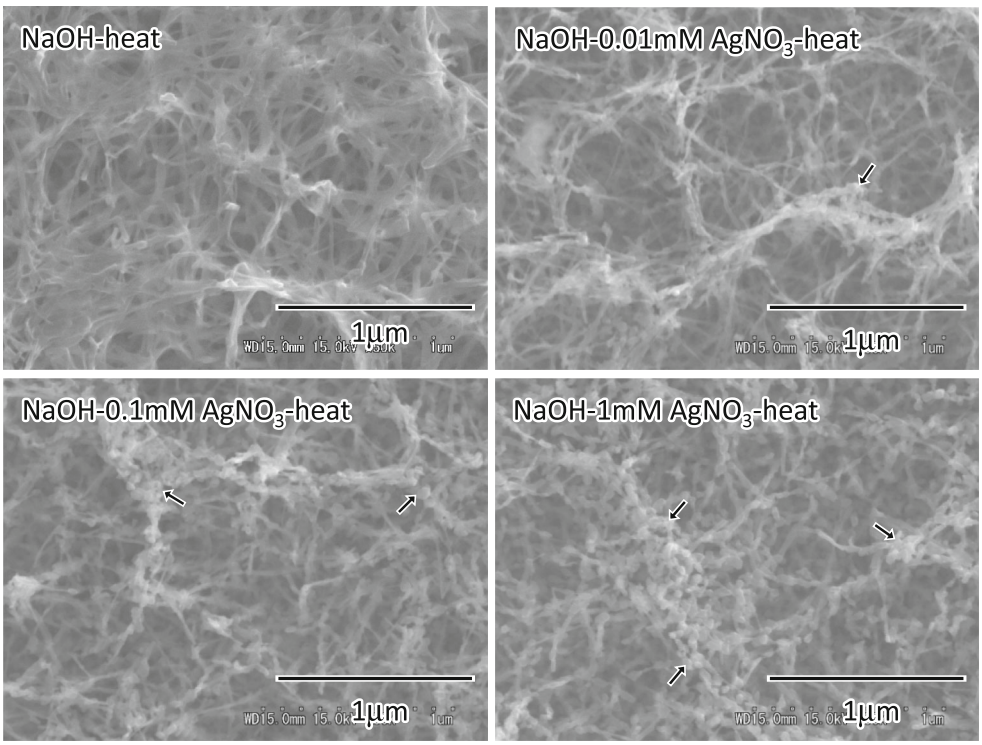

Fig. 1 SEM images of the surfaces of NaOH-heat- and NaOH-$AgNO_3$-heat-treated Ti metals. *Arrows* indicate solid particles

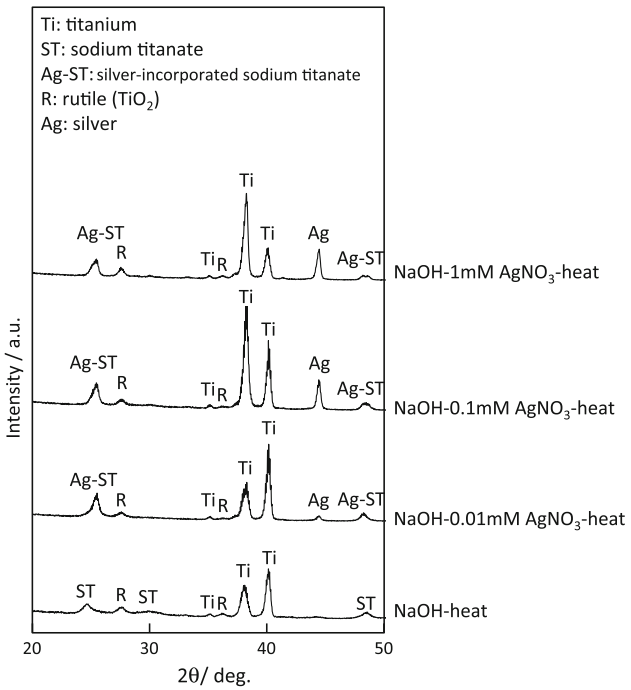

Fig. 2 TF-XRD patterns of the surfaces of NaOH-heat- and NaOH-$AgNO_3$-heat-treated Ti metals

intensity of the diffraction peak ascribed to metallic silver also increased as the concentration of the $AgNO_3$ solution increased.

Table 2 shows the atomic concentrations on the surfaces of the Ti metals and Ti–15Zr–4Nb–4Ta alloy subjected to sequential treatment with NaOH, $CaCl_2$, heat, and $AgNO_3$. Calcium was detected at 3.86 at.% on the surface of the Ti metal subjected to sequential treatment with NaOH, $CaCl_2$, heat, and water. When the NaOH-$CaCl_2$-heat-treated Ti metal was soaked in 0.01–25.0 mM $AgNO_3$ solutions, silver was also detected on the surface, and amount of Ag increased from 0.10 to 1.61 at.% as the concentration of the $AgNO_3$ solution increased from 0.01 to 25.0 mM. The Ti–15Zr–4Nb–4Ta alloy treated with a 1 mM $AgNO_3$ solution contained 0.27 at.% Ag on its surface.

Figure 3 presents SEM images of the surfaces of the Ti metals and the Ti–15Zr–4Nb–4Ta alloy subjected to sequential treatment with NaOH, $CaCl_2$, heat, and $AgNO_3$. All of these Ti metals and the Ti–15Zr–4Nb–4Ta alloy had uniform fine network structures on their surfaces that were similar to the structure observed for the NaOH-heat-treated Ti metal, except the Ti metal subjected to 25 mM $AgNO_3$ treatment, for which aggregates of nanosized particles were observed on the fine network structure.

TF-XRD patterns of the surfaces of the Ti metals subjected to sequential treatment with NaOH, $CaCl_2$, heat, and water or $AgNO_3$ and the Ti–15Zr–4Nb–4Ta alloy subjected to sequential treatment with NaOH, $CaCl_2$, heat, and 1 mM $AgNO_3$ are shown in Fig. 4. The diffraction patterns for all of the Ti metals and the Ti–15Zr–4Nb–4Ta alloy were similar and indicated the formation of only calcium titanate and rutile TiO_2 on their surfaces. Metallic silver was not detected, even on the surfaces of the specimens subjected to 10 mM $AgNO_3$ treatment. Once again, the diffraction

Table 2 Atomic concentrations at the surfaces of Ti metals subjected to sequential treatment with NaOH, $CaCl_2$, heat, and water or $AgNO_3$, and the alloy Ti–15Zr–4Nb–4Ta subjected to sequential treatment with NaOH, $CaCl_2$, heat, and $AgNO_3$

Treatment	Concentration / at.%					
	Ti	Zr + Nb + Ta	O	Na	Ca	Ag
Ti metal						
NaOH-$CaCl_2$-heat-water	26.42 (0.59)	— (—)	69.72 (0.52)	0.00 (0.02)	3.86 (0.17)	0.00 (0.00)
NaOH-$CaCl_2$-heat-0.01 mM $AgNO_3$	27.25 (0.26)	— (—)	70.05 (0.35)	0.00 (0.00)	2.60 (0.05)	0.10 (0.04)
NaOH-$CaCl_2$-heat-0.1 mM $AgNO_3$	27.28 (0.45)	— (—)	68.82 (0.61)	0.00 (0.00)	3.55 (0.23)	0.34 (0.06)
NaOH-$CaCl_2$-heat-1 mM $AgNO_3$	27.08 (0.45)	— (—)	68.63 (0.40)	0.00 (0.00)	3.74 (0.24)	0.55 (0.05)
NaOH-$CaCl_2$-heat-10 mM $AgNO_3$	27.02 (0.77)	— (—)	68.36 (0.53)	0.00 (0.00)	3.80 (0.18)	0.82 (0.22)
NaOH-$CaCl_2$-heat-25 mM $AgNO_3$	25.21 (0.21)	— (—)	68.71 (0.02)	0.00 (0.00)	4.46 (0.14)	1.61 (0.11)
Ti-15Zr-4Nb-4Ta alloy						
NaOH-CaCl-heat-1 mM AgNO	24.39 (0.20)	3.07 (0.23)	69.84 (0.43)	0.00 (0.00)	2.44 (0.09)	0.27 (0.03)

Numbers in parentheses mean SD

peaks ascribed to the calcium titanate shifted slightly to higher diffraction angles with increasing $AgNO_3$ concentration, indicating that all of the introduced silver ions were incorporated into the calcium titanate.

Figure 5 shows AES depth profiles near the surface of the Ti metal subjected to sequential treatment with NaOH, $CaCl_2$, heat, and 1 mM $AgNO_3$. It can be seen from Fig. 5 that the calcium and silver were enriched in the surface layer to a depth of $\sim$1 and 0.5 μm, respectively.

3.2 Apatite formation

SEM images of the surfaces of the Ti metals and Ti-15Zr-4Nb-4Ta alloy soaked in the SBF for 1 day after various chemical and heat treatments can be seen in Fig. 6. The Ti metal subjected to sequential treatment with NaOH, 1 mM $AgNO_3$, and heat was partly covered with aggregates of nanosized particles, while all of the other Ti specimens were fully covered with aggregates. Furthermore, the particles determined to be comprised of apatite via thin-film X-ray diffraction analysis of their surfaces. Notably, the ability of the Ti-15Zr-4Nb-4Ta alloy subjected to sequential treatment with NaOH, $CaCl_2$, heat, and 1 mM $AgNO_3$ to form apatite was slightly lower than that of the correspondingly treated Ti metal.

3.3 Ion release

Figure 7 shows the concentrations of Na and Ca ions released from the Ti metals subjected to NaOH and heat treatment, and NaOH, $CaCl_2$, heat, and water treatments, respectively, into a phosphate buffer solution (KH_2PO_4–K_2HPO_4, pH 7.4) as a function of soaking time. The former released as much as 6 ppm Na^+ ions into the buffer solution within 6 h, while the latter released as little as 0.2 ppm Ca^{2+} ions within the same period of time.

The concentration of Ag ions released into ultrapure water or FBS from the Ti metal subjected to sequential treatment with NaOH, $CaCl_2$, heat, and 1 mM $AgNO_3$ is shown in Fig. 8 as a function of soaking time. While the treated Ti metal released as little as 1.2 ppm Ag ions into water within 10 h, an $\sim$2.7 ppm Ag was detected in the FBS within the same period of time.

The concentrations of Ag ions released into FBS from Ti metals subjected to sequential treatment with NaOH, $CaCl_2$, heat, and $AgNO_3$ solutions with different concentrations, and the Ti–15Zr–4Nb–4Ta alloy subjected to sequential treatment with NaOH, $CaCl_2$, heat, and 1 mM $AgNO_3$ after 24 h are listed in Table 3. The Ag concentration released from the Ti metals increased as the concentration of the used $AgNO_3$ solution increased. In addition, the Ag concentration released from the Ti–15Zr–4Nb–4Ta alloy was less than that released from the correspondingly treated Ti metal.

3.4 Antibacterial activity

The results of the antibacterial activity analyses for the Ti metals subjected to sequential treatment with NaOH and heat; NaOH, $CaCl_2$, heat, and water; NaOH, $CaCl_2$, heat, and 1 mM $AgNO_3$, and the Ti–15Zr–4Nb–4Ta alloy subjected to sequential treatment with NaOH, $CaCl_2$, heat, and 1 mM $AgNO_3$ are presented in Table 4. The antibacterial activity of the Ti metal subjected to sequential treatment with NaOH, $CaCl_2$, heat, and water was extremely low, and slightly lower than that of the Ti metal subjected to only NaOH and heat treatment. Notably, the antibacterial activity of the Ti metal and Ti–15Zr–4Nb–4Ta alloy subjected to sequential treatment with NaOH, $CaCl_2$, heat, and 1 mM $AgNO_3$ was significantly higher.

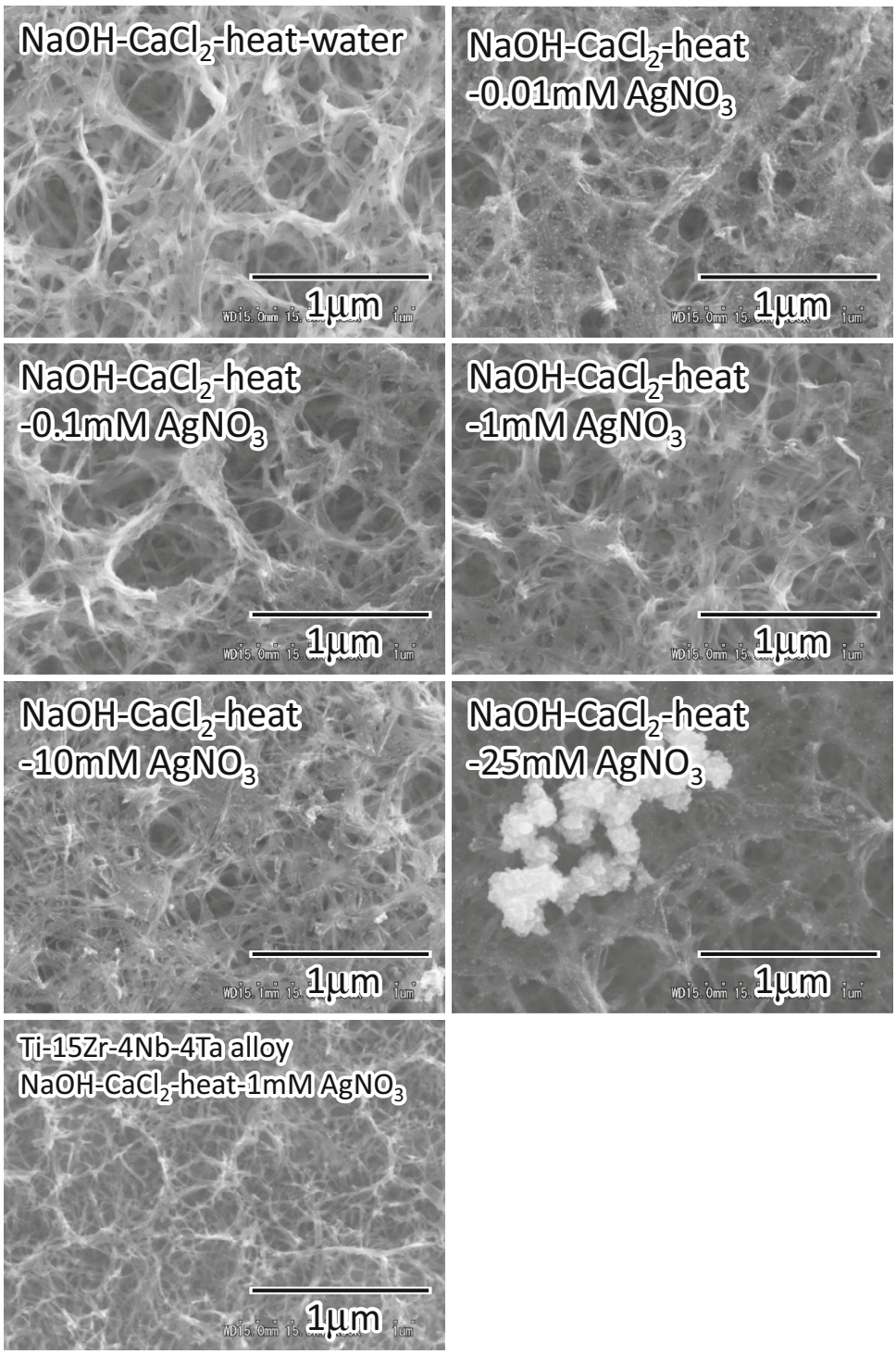

Fig. 3 SEM images of the surfaces of Ti metals subjected to sequential treatment with NaOH, $CaCl_2$, heat, and water or $AgNO_3$ and the alloy Ti-15Zr-4Nb-4Ta subjected to sequential treatment with NaOH, $CaCl_2$, heat, and $AgNO_3$

4 Discussion

Ti metal forms a uniform fine network structure composed of sodium titanate and rutile TiO_2 on its surface following sequential treatment with NaOH and heat, as can be seen in Figs. 1 and 2. Previously [23], we found that this surface layer gradually changes to Ti metal within 1 μm. The Ti metal thus formed with the sodium titanate and rutile TiO_2 on its surface readily formed an apatite layer in SBF, (Fig. 6) and also exhibited slightly higher antibacterial activity (Table 4) than the Ti metal subjected to sequential treatment with NaOH, $CaCl_2$, heat, and water. This

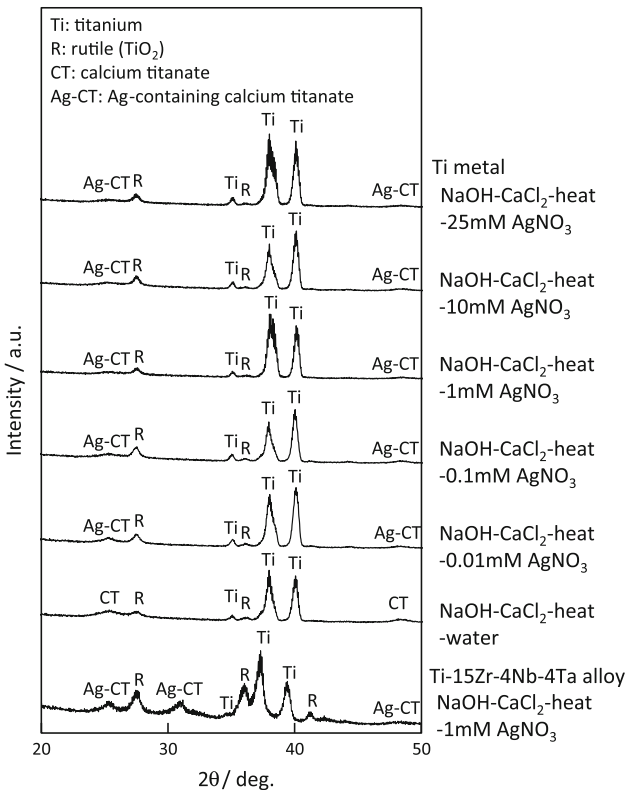

Fig. 4 TF-XRD patterns of the surfaces of Ti metals subjected to sequential treatment with NaOH, $CaCl_2$, heat, and water or $AgNO_3$ and the alloy Ti–15Zr–4Nb–4Ta subjected to sequential treatment with NaOH, $CaCl_2$, heat, and $AgNO_3$

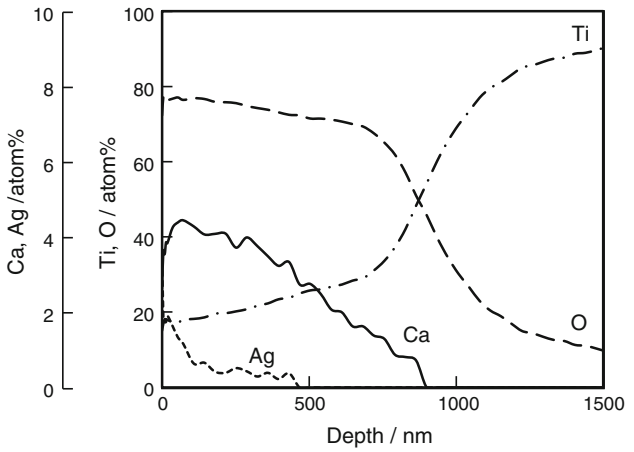

Fig. 5 AES depth profiles near the surface of Ti metal subjected to sequential treatment with NaOH, $CaCl_2$, heat, and 1 mM $AgNO_3$

difference in behavior may be attributed to larger amount of Na^+ ions released into the surrounding fluid by the titanium treated only with NaOH and heat (Fig. 7). The released Na^+ ions may increase the pH of the surrounding fluid and consequently suppress the proliferation of bacteria. However, the antibacterial activity of the NaOH and heat treated Ti was still insufficient.

When Ti metal was subjected to sequential treatment with NaOH, $AgNO_3$ and heat, a uniform fine network structure composed of Ag-containing sodium titanate and rutile TiO_2 was formed on the surface that was essentially similar to the structure observed on the surface of the Ti metal subjected only to NaOH and heat treatment (Figs. 1, 2). As can be seen in Table 1, the concentration of silver ions incorporated into the surface of the Ti metal increased as the concentration of the $AgNO_3$ solution increased. It is thought that most of the Ag ions were incorporated into the layered structure of the sodium titanate [24] via replacement of Na^+ ions because the Na concentration on the surface of the Ti metal decreased and the X-ray diffraction peaks ascribed to sodium titanate shifted to higher diffraction angles with increasing $AgNO_3$ concentration (see Table 1; Fig. 2). The results presented in Table 1 also suggest that incorporation of silver ions into the surface layer of the Ti metal treated with NaOH, $AgNO_3$, and heat reached a maximum at $\sim$2 at.%. However, it is apparent from Figs. 1 and 2 that the introduced silver ions were not only incorporated into sodium titanate but also precipitated as metallic colloids on the surfaces of the Ti metals. These colloidal metallic particles are an issue because they could potentially be released into the living body and cause side effects. In addition, the Ti metal with the Ag-containing sodium titanate on its surface exhibited a lower ability to form an apatite surface layer in SBF than the Ti metal with the Ag-free sodium titanate (Fig. 6). Therefore, the Ti metals with an Ag-containing sodium titanate surface layer are not suitable for implants.

Incorporation of calcium, however, significantly improved the properties of the treated titanium. When Ti metal was subjected to sequential treatment with NaOH, $CaCl_2$, heat, and water, a uniform fine network structure composed of calcium titanate and rutile TiO_2 was observed to form on their surfaces (Figs. 3, 4). Notably, when the Ti metal was soaked in $AgNO_3$ solutions after sequential treatment with NaOH, $CaCl_2$, and heat instead of water, essentially the same uniform fine network structure composed of Ag-containing calcium titanate and rutile TiO_2 was once again observed on the metal surface, except for the specimen treated with 25 mM $AgNO_3$ solution, on which silver colloids precipitated (Figs. 3, 4). Notably, the amount of silver ions incorporated into the surface layer of the Ti metal increased as the concentration of the $AgNO_3$ solution increased (Table 2), and the incorporated silver ions were enriched to a depth of approximately 0.5 μm (Fig. 5). These results indicate that all of the incorporated silver ions were located in the calcium titanate layer, except for the silver ions deposited on the specimen treated with the 25 mM $AgNO_3$ solution, because diffraction peaks

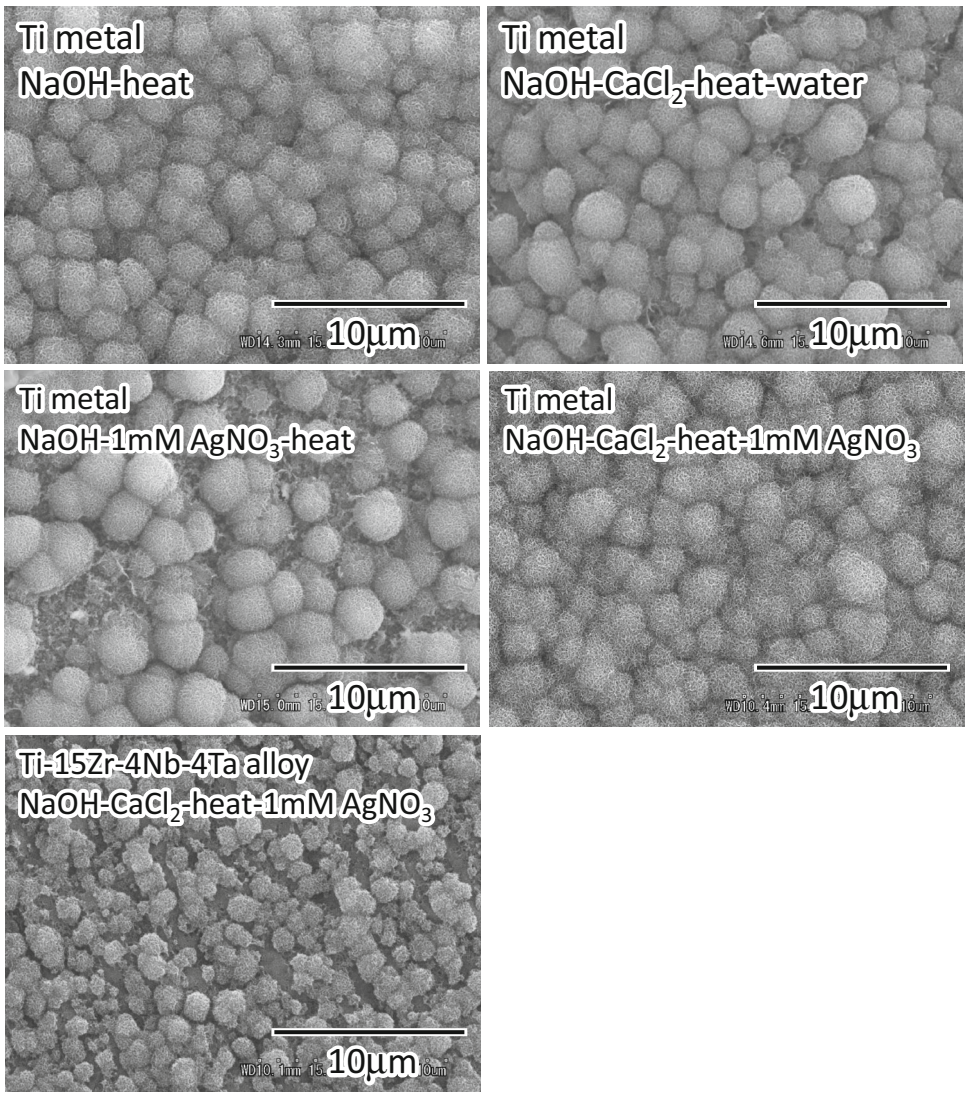

Fig. 6 SEM images of the surfaces of Ti metals subjected to sequential treatment with NaOH and heat; NaOH, $CaCl_2$, heat, and water; NaOH, $CaCl_2$, heat, and 1 mM $AgNO_3$, and of the alloy Ti-15Zr-4Nb-4Ta subjected to sequential treatment with NaOH, $CaCl_2$, heat, and 1 mM $AgNO_3$, after soaking in SBF

other than those ascribed to calcium titanate and rutile TiO_2 were not detected on the surfaces of the treated Ti metals, and the diffraction peaks ascribed to calcium titanate shifted to higher diffraction angles as the concentration of the $AgNO_3$ solution increased. In addition, the silver ions were incorporated into the calcium titanate layer without displacement of calcium ions because the Ca concentration on the surface of the Ti metal did not decrease as the Ag concentration increased (Table 2).

While the Ti metal subjected to sequential treatment with NaOH, $CaCl_2$, heat, and water readily formed an apatite surface layer in SBF (Fig. 6), it had minimal antibacterial activity compared to that of the Ti metal subjected to NaOH and heat treatment (see Table 4). This result may be attributed to the fact that only a minor amount of Ca^{2+} ions were released from the Ti metal into the surrounding fluid (Fig. 7).

On the other hand, the Ti metals subjected to sequential treatment with NaOH, $CaCl_2$, heat, and $AgNO_3$ slowly released considerable amounts of silver ions into water and FBS (Fig. 8), and the amount of released silver ions was proportional to the concentration of the $AgNO_3$ solution used to soak the samples (Table 3). Furthermore, the silver ions were more readily released into FBS than water because the released silver ions tended to combine with proteins in the FBS to form various complexes. Due to this greater release of silver ions, the Ti metals subjected to sequential treatment with NaOH, $CaCl_2$, heat, and $AgNO_3$ exhibited considerably high antibacterial activity (Table 4).

Furthermore, the Ag-treated Ti metals readily formed apatite surface layers in SBF and exhibited behavior nearly equal to that of the Ag-free bioactive Ti metals prepared via treatment with just NaOH and heat or NaOH, $CaCl_2$, heat, and water (Fig. 6).

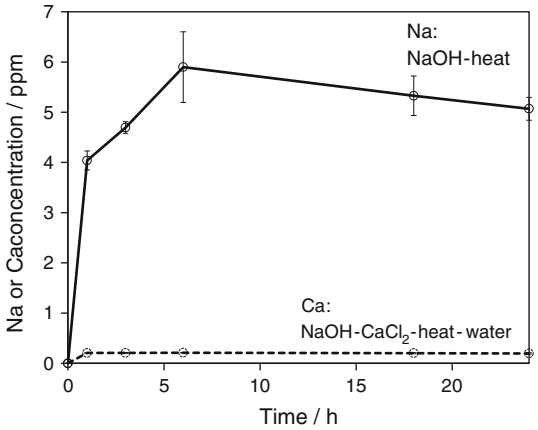

Fig. 7 Concentration of Na and Ca ions released into PBS as a function of soaking time from NaOH-heat- and NaOH-$CaCl_2$-heat water treated Ti metals

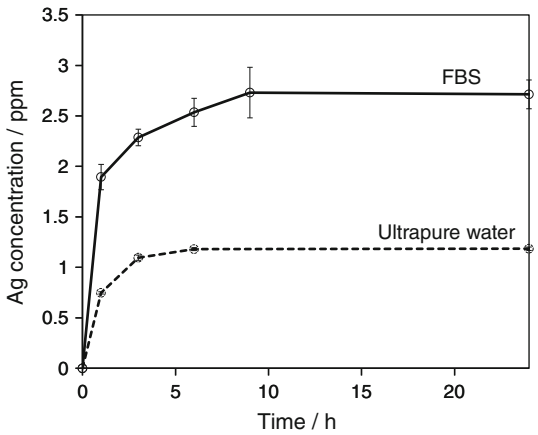

Fig. 8 Concentration of Ag ions released into ultrapure water and FBS from Ti metal subjected to sequential treatment with NaOH, $CaCl_2$, heat, and 1 mM $AgNO_3$

Finally, like the Ti metal, the surface layer of the Ti–15Zr–4Nb–4Ta alloy subjected to sequential treatment with NaOH, $CaCl_2$, heat, and $AgNO_3$ was also enriched with Ag^+ and Ca^{2+} ions (Table 2), released a considerable amount of Ag^+ ion into FBS (Table 3), and exhibited both high antibacterial activity (Table 4) and a fairly high ability to form an apatite surface layer in SBF (Fig. 6); however, the amount Ag^+ ions (Table 2) incorporated into the treated alloy and its ability to form an apatite surface layer (Fig. 6) were slightly lower than those of the correspondingly treated Ti metal.

Based on these results, the Ti metal and Ti alloys subjected to sequential treatment with NaOH, $CaCl_2$, heat, and $AgNO_3$ are believed to have significant potential for the production of various types of dental and orthopedic implants, because they may exhibit high antibacterial activity and excellent bone-bonding properties in vivo.

Table 3 Ag ion concentration of FBS in which the Ti metal and Ti alloy subjected to sequential treatment with NaOH, $CaCl_2$, heat, and $AgNO_3$ were soaked for 24 h

Treatment	Ag^+ ion concentration of FBS/ppm
Ti metal	
NaOH-$CaCl_2$-heat-0.01 mM $AgNO_3$	0.35
NaOH-$CaCl_2$-heat-0.1 mM $AgNO_3$	0.80
NaOH-$CaCl_2$-heat-1 mM $AgNO_3$	2.66
NaOH-$CaCl_2$-heat-10 mM $AgNO_3$	3.24
Ti–15Zr–4Nb–4Ta alloy	
NaOH-$CaCl_2$-heat-1 mM $AgNO_3$	1.45

Table 4 Antibacterial test results

Sample	Average of *St. aureus* count/CFU		Antibacterial activity value
	After inoculation	After incubation	
Ti metal			
NaOH-heat	1.8×10^6	5.7×10^7	0.8
NaOH-$CaCl_2$-heat-water	2.8×10^5	5.2×10^8	0.1
NaOH-$CaCl_2$-heat-1 mM $AgNO_3$	8.2×10^5	<20	7.2
Ti-15Zr-4Nb-4Ta alloy			
NaOH-$CaCl_2$-heat-1 mM $AgNO_3$	1.9×10^5	<20	8.1

5 Conclusion

Ti metal and the alloy Ti–15Zr–4Nb–4Ta were prepared with Ag-containing calcium titanate layers on their surfaces via sequential NaOH, $CaCl_2$, heat, and $AgNO_3$ treatment. In addition to possessing the ability to form an apatite surface layer in SBF, the Ti materials slowly released silver ions and exhibited high antibacterial activity. Therefore, these surface-modified metals are believed to be useful for the production of various types of dental and orthopedic implants.

References

1. Kim H-M, Miyaji F, Kokubo T, Nakamura T. Preparation of bioactive Ti and its alloys via simple chemical surface treatment. J Biomed Mater Res. 1996;32:409–17.
2. Yan W-Q, Nakamura T, Kobayashi M, Kim H-M, Miyaji F, Kokubo T. Bonding of chemically treated titanium implants to bone. J Biomed Mater Res. 1997;37:267–75.
3. Nishiguchi S, Fujibayashi S, Kim H-M, Kokubo T, Nakamura T. Biology of alkali- and heat-treated titanium metal. J Biomed Mater Res. 2003;67A:26–35.

4. Kizuki T, Takadama T, Matsushita T, Nakamura T, Kokubo T. Preparation of bioactive Ti metal surface enriched with calcium ions by chemical treatment. Acta Biomater. 2010;6:2836–42.
5. Yamaguchi S, Takadama H, Matsushita T, Nakamura T, Kokubo T. Apatite-forming ability of Ti–15Zr–4Nb–4Ta alloy induced by calcium solution treatment. J Mater Sci Mater Med. 2010;21:439–44.
6. Fukuda A, Takemoto M, Saito T, Fujibayashi S, Neo M, Yamaguchi S, Kizuki T, Matsushita T, Niinomi M, Kokubo T, Nakamura T. Bone bonding bioactivity of Ti metal and Ti–Zr–Nb–Ta alloys with Ca ions incorporated on their surfaces by simple chemical and heat treatment. Acta Biomater. 2011;7:1379–86.
7. Kawanabe K, Ise K, Goto K, Akiyama H, Nakamura T, Kaneuji A, Sugimori T, Matsumoto T. A new cementless total hip arthroplasty with bioactive titanium porous-coating by alkaline and heat treatment: average 4.8-year result. J Biomed Mater Res. 2009;90B:476–81.
8. So K, Kaneuji A, Matsumoto T, Matsuda S, Akiyama H. Is the bone-bonding ability of a cementless total hip prosthesis enhanced by alkaline and heat treatment? Clin Orthop Relat Res. 2013;471(12):3847–55.
9. Hamilton H, Jamieson J. Deep infection in total hip arthroplasty. Can J Surg. 2008;51:111–7.
10. Hu S, Chang J, Liu M, Ning C. Study on antibacterial effect of 45S5 Bioglass. J Mater Sci Mater Med. 2009;20:281–6.
11. Zhang D, Leppäranta O, Munukka E, Ylänen H, Viljanen MK, Eerola E, Hupa M, Hupa L. Antibacterial effects and dissolution behavior of six bioactive glasses. J Biomed Mater Res. 2010;93A:475–83.
12. Chen Y, Zheng X, Xie Y, Ji H, Ding C, Li H, Dai K. Silver release from silver-containing hydroxyapatite coatings. Surf Coat Tech. 2010;205:1892–6.
13. Lu X, Zhang B, Wang Y, Zhou X, Weng J, Qu S, Feng B, Watari F, Ding Y, Leng Y. Nano-Ag-loaded hydroxyapatite coatings on titanium surfaces by electrochemical deposition. J R Soc Interface. 2010;6:1–11.
14. Qu J, Lu X, Li D, Ding Y, Leng Y, Weng J, Qu S, Feng B, Watari F. Silver/hydroxyapatite composite coatings on porous titanium surfaces by sol-gel method. J Biomed Mater Res Part B. 2011;97B:40–8.
15. Chen W, Liu Y, Courtney HS, Bettenga M, Agrawal CM, Bumgardner JD, Ong JL. In vitro anti-bacterial and biological properties of magnetron co-sputtered silver-containing hydroxyapatite coating. Biomater. 2006;27:5512–7.
16. Miola M, Ferraris S, Di Nunzio S, Robotti PF, Bianchi G, Fucale G, Maina G, Cannas M, Gatti S, Massé A, Vitale Brovarone C, Vern E. Surface silver-doping of biocompatible glasses to induce antibacterial properties. Part II; plasma sprayed glass-coatings. J Mater Sci Mater Med. 2009;20:741–9.
17. Noda I, Miyaji F, Ando Y, Miyamoto H, Shimazaki T, Yonekura Y, Miyazaki M, Mawatari M, Hotokebuchi T. Development of novel thermal sprayed antibacterial coating and evaluation of release properties of silver ions. J Biomed Mater Res Part B. 2009;89B:456–65.
18. Stigter M, de Groot K, Layrolle P. Incorporation of tobramycin into biomimetic hydroxyapatite coating on titanium. Biomater. 2002;23:4143–53.
19. Inoue Y, Uota M, Torikai T, Watari T, Noda I, Hotokebuchi T, Yada M. Antibacterial properties of nanostructured silver titanate thin films formed on a titanium plate. J Biomed Mater Res. 2010;92A:1171–80.
20. Yada M, Inoue Y, Akihito G, Noda I, Torikai T, Watari T, Hotokebuchi T. Apatite-forming ability of titanium compound nanotube thin films formed on a titanium metal plate in a simulated body fluid. Col Surf B. 2010;80:116–24.
21. Kokubo T, Yamaguchi S. Bioactive Ti metal and its alloys prepared by chemical treatments: state-of-the-art and future trends. Adv Eng Mater. 2010;12:B579–91.
22. Kokubo T, Takadama H. How useful is SBF in predicting in vivo bone bioactivity? Biomater. 2006;27:2907–15.
23. Yamaguchi S, Takadama H, Matsushita T, Nakamura T, Kokubo T. Cross-sectional analysis of the surface ceramic layer developed on Ti metal by NaOH-heat treatment and soaking in SBF. J Ceram Soc Japan. 2009;117:1126–30.
24. Margad JrE, de Abreu MAS, Pravia ORC, Marinkovic BA, Jardim PM, Rizzo FC, Araújo AS. A study on the structure and thermal stability of titanate nanotubes as a function of sodium content. Solid State Sci. 2006;8:888–900.